

# Morphogenesis of chicken liver: identification of localized growth zones and the role of $\beta$ -catenin/Wnt in size regulation

Sanong Suksaweang, Chih-Min Lin, Ting-Xin Jiang, Michael W. Hughes, Randall B. Widelitz, and Cheng-Ming Chuong\*

*Department of Pathology, Keck School of Medicine, University of Southern California, Los Angeles, CA 90033, USA*

Received for publication 10 April 2003, revised 10 September 2003, accepted 7 October 2003

## Abstract

During development and regeneration, new cells are added and incorporated to the liver parenchyma. Regulation of this process contributes to the final size and shape of the particular organs, including the liver. We identified the distribution of liver growth zones using an embryonic chicken model because of its accessibility to experimentation. Hepatocyte precursors were first generated all over the primordia surrounding the vitelline blood vessel at embryonic day 2 (E2), then became limited to the peripheral growth zones around E6. Differentiating daughter cells of the peripheral hepatocyte precursors were shown by DiI microinjection to be laid inward and were subsequently organized to form the hepatic architecture. At E8, hepatocyte precursor cells were further restricted to limited segments of the periphery, called localized growth zones (LoGZ). Adhesion and signaling molecules in the growth zone were studied. Among them,  $\beta$ -catenin and Wnt 3a were highly enriched. We overexpressed constitutively active  $\beta$ -catenin using replication competent avian sarcoma (RCAS) virus. Liver size increased about 3-fold with an expanded hepatocyte precursor cell population. In addition, blocking  $\beta$ -catenin activity by either overexpression of dominant-negative LEF1 or overexpression of a secreted Wnt inhibitor Dickkopf (DKK) resulted in decreased liver size with altered liver shape. Our data suggest that (1) the duration of active growth zone activity modulates the size of the liver; (2) a shift in the position of the localized growth zone helps to shape the liver; and (3)  $\beta$ -catenin/Wnt are involved in regulating growth zone activities during liver development.

© 2003 Elsevier Inc. All rights reserved.

*Keywords:* Hepatocyte progenitor cells; Hepatogenesis; Stem cell; Gene therapy; Regeneration

## Introduction

Epithelial–mesenchymal interactions are essential for induction, morphogenesis, differentiation, and regeneration in all epithelial organs (review in Chuong, 1998; Hogan, 1999). This holds true for the liver. During induction, the future hepatic endoderm (ventral gut endoderm) is specified by several growth factors produced by the cardiac mesoderm, such as fibroblast growth factor 1 (FGF1), FGF2, and

possibly FGF8 (Jung et al., 1999). Recently, this specification was also found to require bone morphogenetic proteins (BMPs) in the cardiac mesoderm and septum transversum (Rossi et al., 2001). However, the mechanism regulating the size and shape of the liver after induction has not been clearly elucidated.

After the induction stage, hepatocytes and biliary cells form from multipotent endodermal hepatoblasts (reviewed in Vessey and Hall, 2001; Zaret, 2000, 2002). The specified hepatic endoderm proliferates and forms hepatic cords (Carlson, 1999; Zaret, 2002, Fig. 1). These cords constitute the liver parenchyma after differentiation and acquisition of liver-specific gene expression. The hepatic cord is the building unit of the liver and its formation is pivotal to chemical processing, metabolism, and serum protein-production functions of the liver.

The liver is made of lobes with specific shapes and sizes. The size of the liver is tightly controlled during

*Abbreviations:* LoGZ, localized growth zones; RCAS, replication competent avian sarcoma; PCNA, proliferating cell nuclear antigen; L-CAM, Liver cell adhesion molecule; AER, apical ectodermal ridge; FGFs, fibroblast growth factors.

\* Corresponding author. Department of Pathology, Keck School of Medicine, University of Southern California, HMR 315B, 2011 Zonal Avenue, Los Angeles, CA 90033. Fax: +1-323-442-3049.

*E-mail address:* [chuong@pathfinder.usc.edu](mailto:chuong@pathfinder.usc.edu) (C.-M. Chuong).

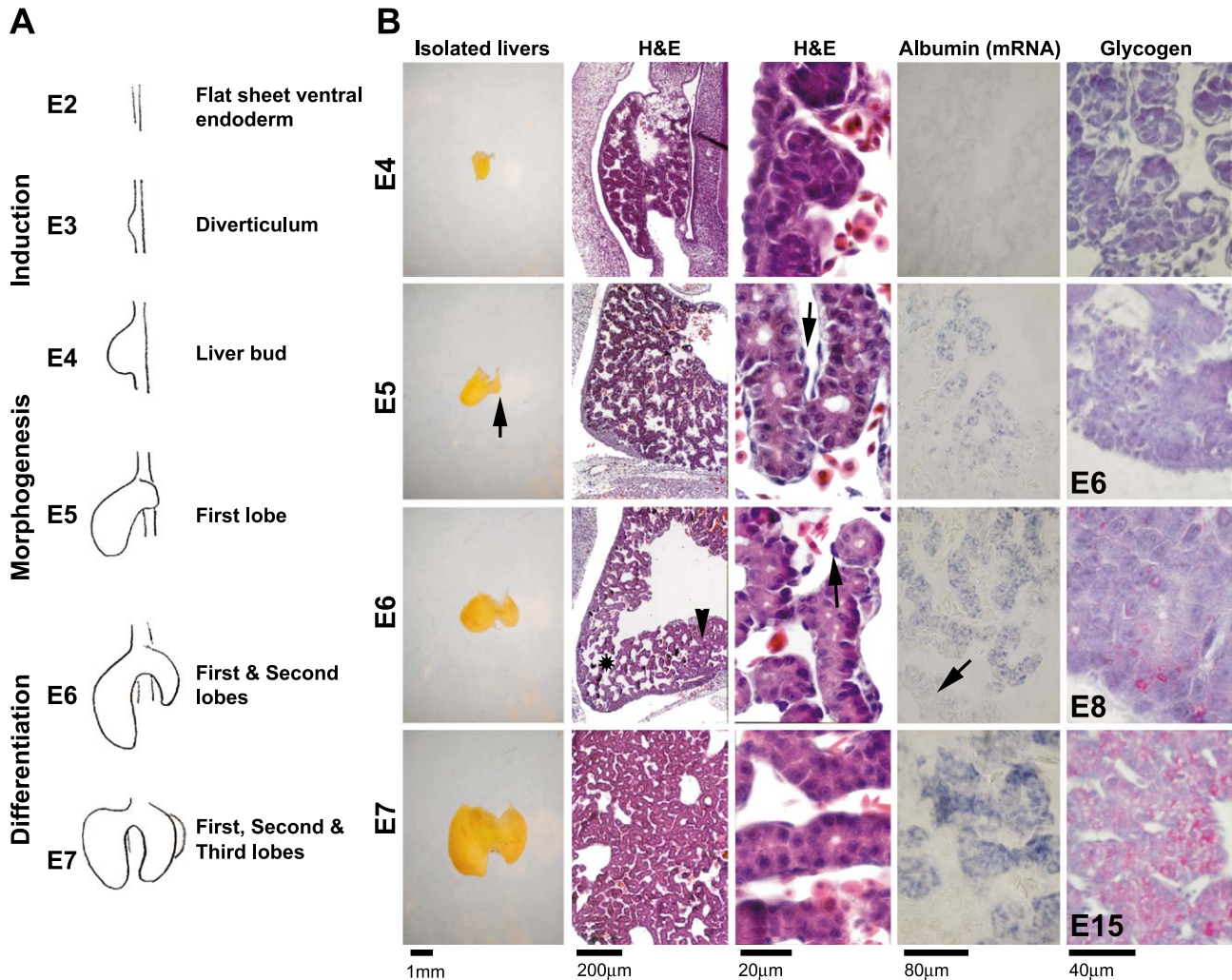


Fig. 1. Development of the chicken liver. (A) Schematic drawing of chicken liver development. (B) Liver morphology shown in the isolated livers, the H&E sections at 10× (H&E left column) and 100× (H&E right column) from E4 to E7, the in situ hybridization of albumin-mRNA of corresponding stages at 20× (Albumin), and the glycogen expression detected by PAS staining from E4, E6, E8, and E15, respectively (Glycogen). The H&E staining shows the progression of the hepatocytes forming the hepatic cords as the liver grows. E5, isolated liver, arrow indicates newly formed second lobe. E5, H&E, arrow indicates endothelium. E6, H&E, asterisk indicates large sinusoids in growing tip. Arrowhead indicates smaller sinusoids. Arrow indicates endothelium. E6, Albumin, arrow indicates liver periphery.

development through adulthood. The size can be restored after injury or loss (e.g., partial hepatectomy) by regenerative processes within 10 days (Michalopoulos, 1990; Monga et al., 2001). During medical intervention, repopulation of hepatocytes may be achieved by hepatocyte transplantation, bone marrow transplantation (Wang et al., 2002), or stem cell transplantation. Understanding the regulation of morphogenesis and hepatocyte repopulation is important but the mechanisms have not been evaluated yet.

The Wnt/ $\beta$ -catenin pathway has been shown to regulate multiple cell properties controlling morphogenesis, such as growth, axial polarity determination, and apoptosis. The accumulation of  $\beta$ -catenin leads to uncontrolled cell growth implicated in a broad range of tumors, such as hepatocellular carcinoma (HCC), breast cancer, lung cancer, ovarian cancer, colon cancer, synovial carcinoma, etc. (Polakis,

2000, Saito et al., 2000).  $\beta$ -Catenin plays a central role mediating the canonical Wnt/ $\beta$ -catenin signaling pathway (Jeng et al., 2000). A chicken  $\beta$ -catenin homolog was cloned (Lu et al., 1997) and ectopic expression of constitutively active  $\beta$ -catenin caused avian foot scale epidermis to grow feathers (Widelitz et al., 2000). This suggests its possible role in specifying cellular fates. Furthermore, alterations (missense mutations or interstitial deletions) of this gene are associated with hepatoblastoma (Wei et al., 2000). However, the fundamental function of  $\beta$ -catenin in early liver growth has not been established. During liver regeneration, it is one of the earliest affected genes, induced within 5 min (Monga et al., 2001). Therefore, it is important to investigate its expression and function during early liver development.

To study this, we chose the chicken liver as a model because of its remarkable accessibility to experimentation,

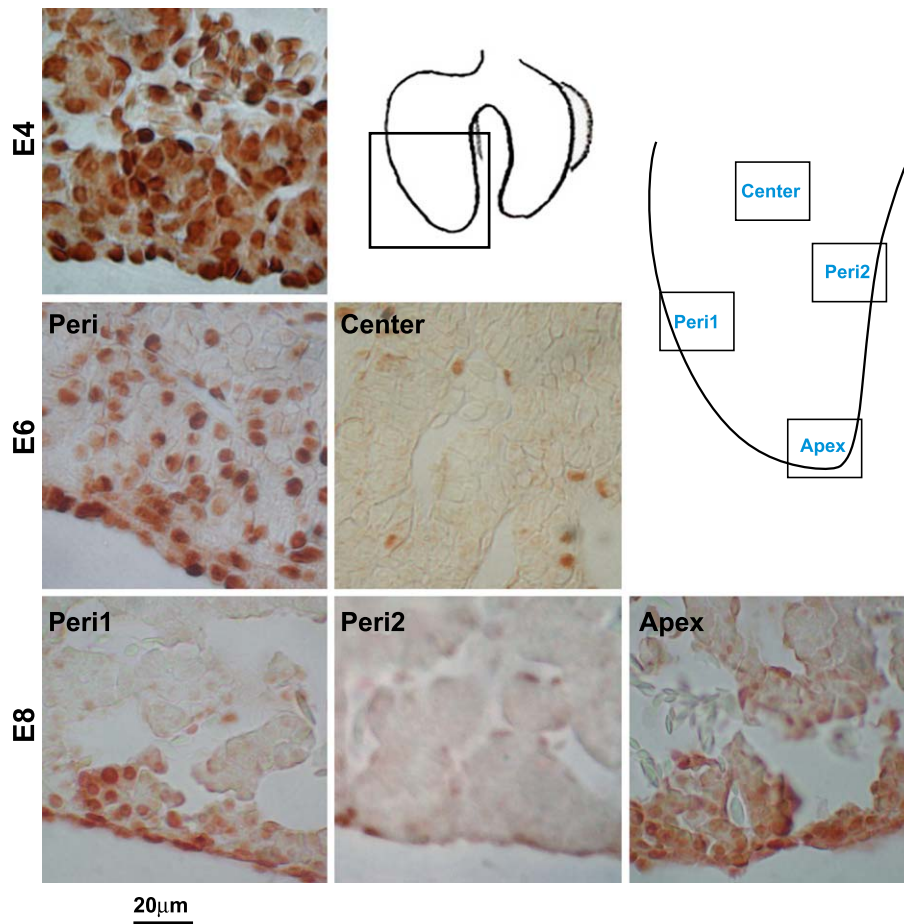


Fig. 2. Identification of the LoGZ during liver development. Immunohistochemistry of PCNA staining at E4, E6, and E8. PCNA is all over in early liver stages but becomes restricted to several localized growth zones in the periphery and apex at later stages. Schematic drawings show the locations of the panels taken. Peri (periphery) 1 represents localized growth zones. Peri2 represents regions without growth zone activity. Scale bars, 20  $\mu$ m.

in which molecules or chemicals can be added in ovo. At early developmental stages, embryos are transparent facilitating microinjections. We hypothesize that regulation of localized growth zone activities during liver morphogenesis gives rise to the mass and shape of the liver. To test this, we examined the location of proliferating cells in embryonic livers by staining for proliferating cell nuclear antigen (PCNA) at various times during liver development. We sought to study the molecular microenvironments that orchestrate the activity of the growth zone. In this study, we showed that  $\beta$ -catenin played a crucial role. Its dynamic expression pattern coincides with that of the localized growth zones (LoGZ). Overexpression of a constitutively active  $\beta$ -catenin resulted in an expanded population of hepatocyte precursors and increased liver size. Furthermore, blocking its activity by overexpressing a dominant-negative LEF1 led to a decreased liver size. In addition, blockage of the canonical pathway by administration of DKK (Glinka et al., 1998) dramatically changed the size and shape of the liver. Understanding the molecular regulation of early liver development may help gain new insights into liver pathogenesis and aid in

identifying potential targets for future therapy to curtail liver diseases.

## Materials and methods

### *Histology and immunohistochemistry and in situ hybridizations*

Embryos were sectioned to 5–6  $\mu$ m and stained for H&E and immunohistochemistry as described (Jiang et al., 1998) with a few modifications. Immunohistochemistry was done using the automated Ventana Discovery™ system. Blocking solution contained 10% FBS/0.5% BSA in PBS. Antibody dilution solution contained 2% FBS/0.1% BSA. The antibodies were anti- $\beta$ -catenin (Sigma), anti-L-CAM, anti-PCNA (Chemicon), anti-tenascin-C (M1B4), anti-p19 (AMV-3C2) and anti-vimentin (H5) (developed by Fambrough and obtained from the Developmental Studies Hybridoma Bank developed under the auspices of the NICHD and maintained by Department of Biological Sciences, The University of Iowa, Iowa City, IA 52242),

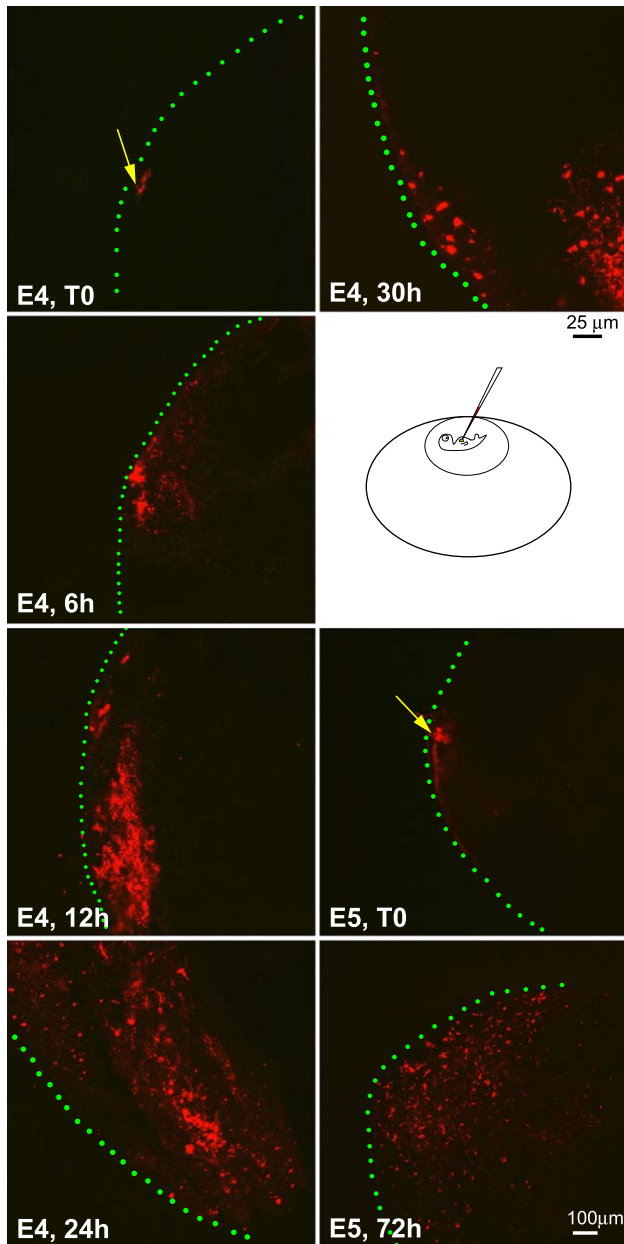


Fig. 3. Use of DiI labeling to trace the lineages of cells in the localized growth zones. E4 and E5 embryo livers were labeled with lipophilic-fluorescent dye DiI and the livers were isolated at specified time points. Specimens were collected at time zero (T0), 6, 12, 24, 30, and 72 h, respectively. The liver specimens were observed with a confocal microscope. The pictures represent the maximum projection, in which all the planes (X, Y, and Z) are combined by computerization. Injection sites were marked with a yellow arrow and the surface of the liver lobe with green lines. As time progresses, labeled cells become more widely and inwardly distributed. Note that a few labeled cells remain at the injection site. Size bar is 25  $\mu\text{m}$  for E4 and 100  $\mu\text{m}$  for E5. The microinjection diagram was not drawn to scale.

anti-c-Myc (Research Diagnostic), and anti-HA (Santa Cruz).

Whole mount and section in situ hybridizations were used to detect mRNA levels from chicken embryos at different H&H stages (Hamburger and Hamilton, 1951). The whole

mount in situ protocol was performed as described (Jiang et al., 1998). Some section in situ hybridization was performed using the automated Discovery™ system (Ventana Medical System) with recommended protocols.

#### *Reverse transcription-polymerase chain reaction*

mRNA was extracted with the RNeasy Protection kit (Qiagen). AMV reverse transcriptase (Roche Diagnostics) was used for reverse transcription (RT) and polymerase chain reaction (PCR) was performed using the protocol recommended by the manufacturer (Panvera). Primers used in Fig. 5 are as follows: replication competent avian sarcoma (RCAS) (a = sense: AGCCTGAAAGCAGAATA; b = antisense: GCAAGACTACAACAGTA),  $\beta$ -catenin (c = sense: ATGGCAATCAAGAAAGTAAGC; d = antisense: GTACAACAACAGTGCACAAATAG), and GAPDH (e = sense: GGCGAGATGGTGAAAGTCG; f = antisense: CAGTTGGTGGTGCACGATG).

#### *DiI injection*

To trace liver cell movement during morphogenesis, E4 and E5 embryos were exposed. Lipophilic dye (1–2  $\mu\text{l}$ ) was microinjected into the surface of liver buds of different embryos in a reproducible way (checked by examining sections at time 0). Livers were isolated every 6 h after labeling. The isolated livers were fixed in 4% PFA at 4°C for 16–18 h, washed in PBS twice for 5 min. The livers were kept in the dark until their fluorescence was monitored by confocal microscopy [The Microscopy Sub core at the USC Center for Liver Diseases (NIH 1 P03 DK48522)]. Each time point presents a representative liver from three or four specimens.

#### *Periodic acid Schiff (PAS) staining*

To verify hepatocyte differentiation status, glycogen was detected using the PAS method (Warren and Hamilton, 1981) as recommended by the manufacturer (Sigma). Briefly, sections were deparaffinized, rehydrated, and immersed in Periodic Acid Solution for 5 min at room temperature (18–25°C). Slides were then rinsed and immersed in Schiff's reagent for 15 min, counterstained with Hematoxylin Solution (Gill No.3), dehydrated, cleared, and mounted.

#### *RCAS viral production*

RCAS-truncated *Xenopus*  $\beta$ -catenin lacking the amino and carboxy termini was provided by Dr. Johnson (Capdevila et al., 1998). Virus was prepared as described (Jiang et al., 1998). Increased viral titers were obtained from supernatants after centrifugation at 12,000 rpm for 30 min before the injection. RCAS-DKK was constructed using the RCAS Gateway system (Loftus et al., 2001).

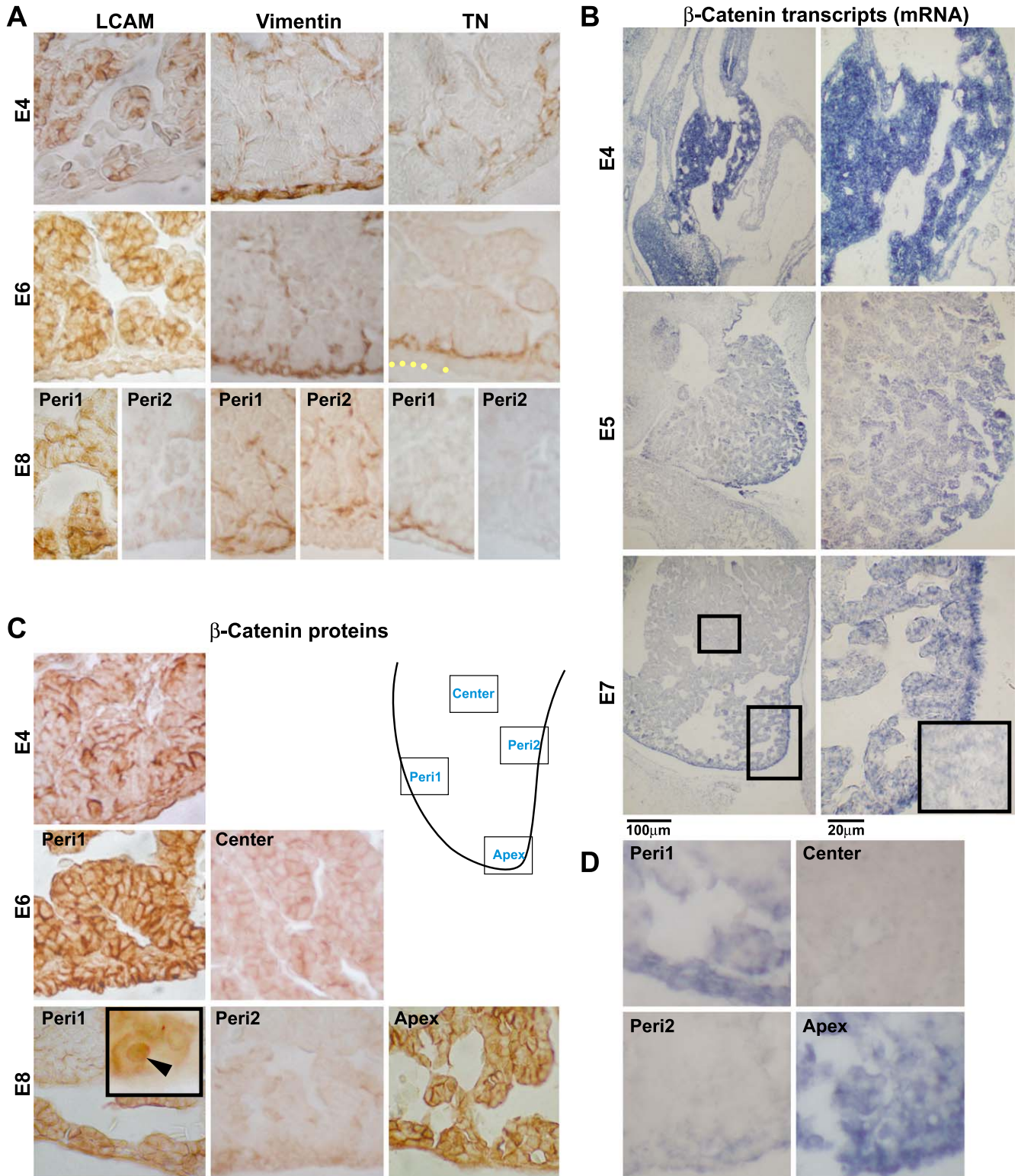


Fig. 4. Molecular expression during hepatogenesis. (A) Immunohistochemical localization of L-CAM, vimentin, and tenascin-C at E4, E6, and E8. (B) The expression of  $\beta$ -catenin transcripts at E4, E5, and E7. The inset in (B) at E7 was a higher magnification view of the center of the liver lobe from the left column. (C) The expression pattern of  $\beta$ -catenin proteins at E4, E6, and E8, respectively. The nuclear staining was observed (inset). (D) The expression of Wnt 3a transcripts at E7. Each of these micrographs was chosen as representative from at least three independent samples. Panels A and C are immunohistochemistry and brown colors are positive. B and D are in situ hybridization and blue colors are positive. Peri1 represents localized growth zones and Peri2 represents regions without growth zone activity as shown in the schematic drawing. Note the difference in the expression patterns in the parenchymal center, Peri1, and Peri2. Scale bar, 20 and 100  $\mu$ m.

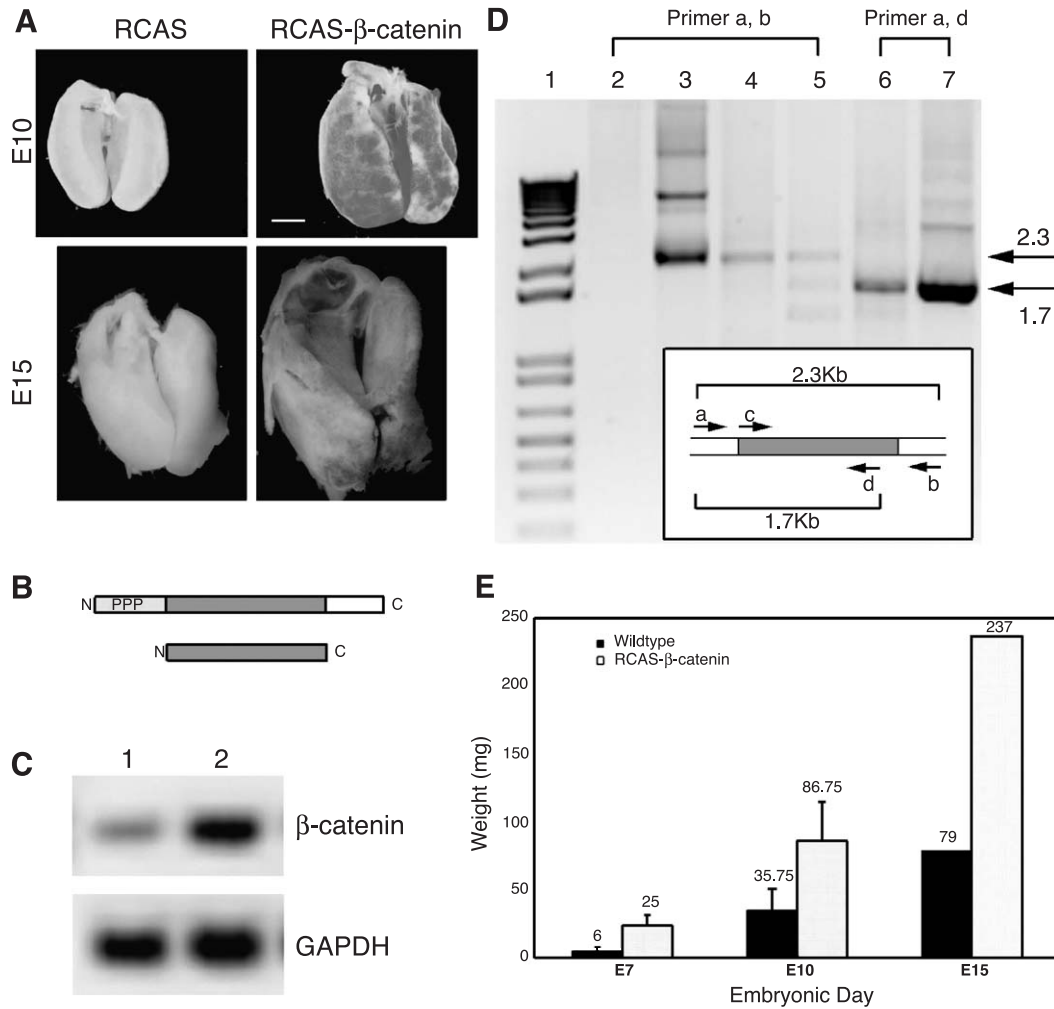


Fig. 5. Effects of overexpressing  $\beta$ -catenin in developing chicken liver. (A) RCAS-control and RCAS- $\beta$ -catenin transduced livers were isolated at E10 (upper row) and E15 (lower row), respectively. Scale bar, 1 mm. (B) Upper diagram of wild type with phosphorylation sites (light grey, PPP), armadillo repeats (grey), and cytoplasmic tail (blank) and lower diagram of constitutively active  $\beta$ -catenin, lacking N- and C-termini. (C) RT-PCR of  $\beta$ -catenin and glyceraldehydes 3-phosphate dehydrogenase (GAPDH) for the control (1) and affected (2) livers. (D) Transduction of RCAS- $\beta$ -catenin was further verified by two sets of RT-PCR experiments. cDNAs in lanes 2–5 were amplified with RCAS primers. cDNAs in lanes 6–7 were amplified with sense-RCAS and antisense- $\beta$ -catenin primers. The size of the PCR products from the wild type and truncated  $\beta$ -catenin are indicated (arrows). Lane 1, molecular weights markers; lane 2, wild-type liver cDNA; lane 3, RCAS- $\beta$ -catenin plasmid; lane 4, affected liver cDNA; lane 5, affected limb cDNA; lane 6, affected liver cDNA; lane 7, RCAS- $\beta$ -catenin plasmid. The inset is a diagram representing the RCAS- $\beta$ -catenin plasmid and the primers used for PCR. (E) The change of liver weights was quantified. The means of the liver weights at E7 ( $n = 3$ ), E10 ( $n = 4$ ), and E15 ( $n = 1$ ) were graphed ( $P < 0.05$ ; paired  $t$  test).

### *In ovo microinjection*

Each egg was sterilized with 70% ethanol and a 15- to 20-mm-diameter window was made. Stages 20–21 embryos were microinjected with 5–10  $\mu$ l of virus into the body cavity between the developing heart and gizzard. The windows were closed with scotch tape and the eggs were placed back into the humidified incubator for three or more days.

### *Luciferase reporter gene assays*

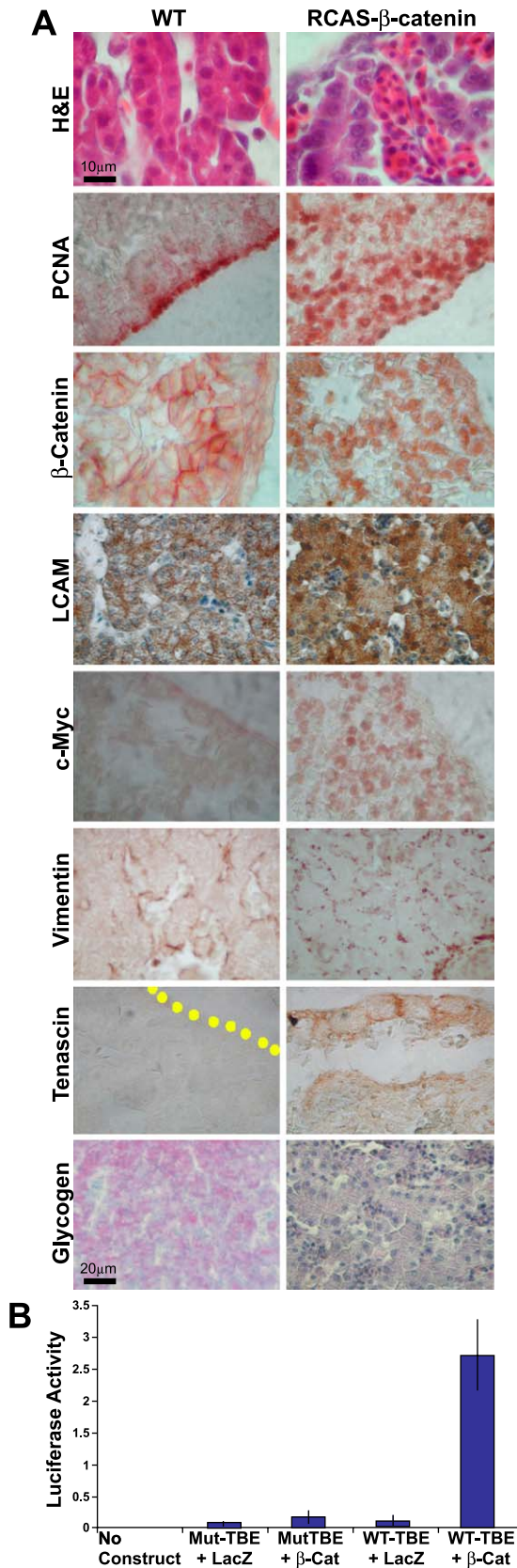
E6 liver cells (50,000) were plated in 24-well plates 16–18 h before transfection. Transfections were performed as described with Targefect F2 (Targeting systems) following

the procedures recommended by the manufacturer.  $\beta$ -Catenin activity was assessed using a TCF-4 binding element (TBEs) directing expression of luciferase (He et al., 1998).

## Results

### *The development of chicken liver and expression of molecular markers*

Stages of liver development from E4 to E7 are shown in schematic representations (Fig. 1A). We examined the livers from E4 to E7 (Fig. 1B). At E4 (H&H stage 24), the newly formed liver primordium was identified microscopically as a small, yellow-white bud adjacent to the heart and gizzard,



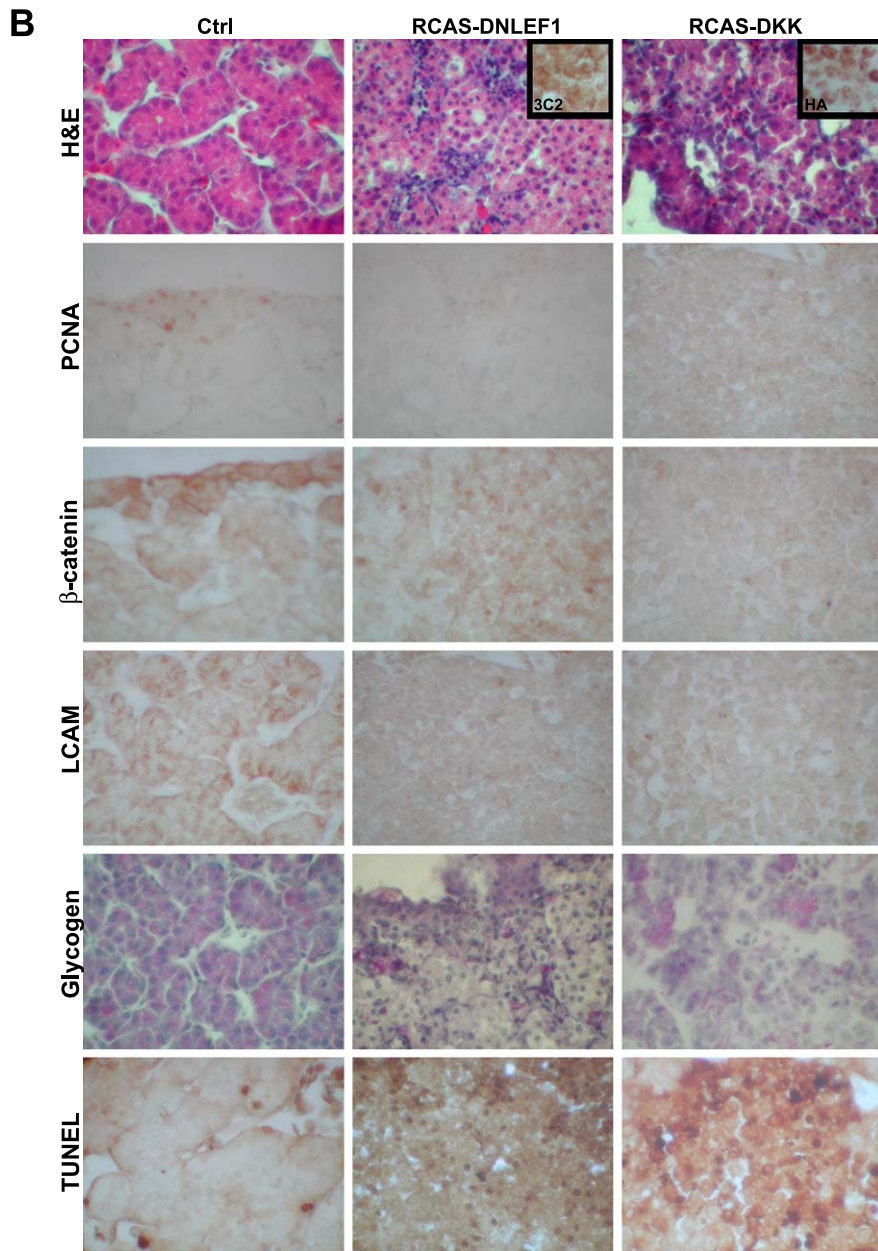
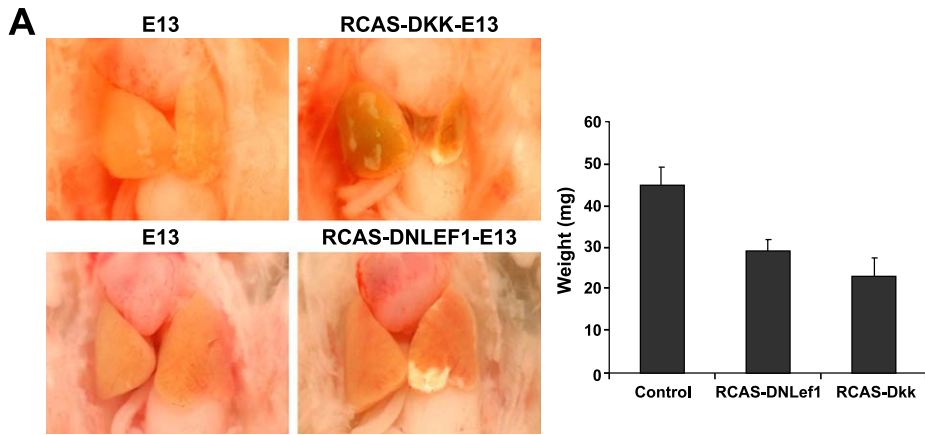
situated to the right of the spinal cord. This liver primordium was composed of loosely arranged hepatocyte precursor cells (Fig. 1B, H&E). The parenchymal cells expressed extremely low levels of albumin, undetectable by in situ hybridization (Fig. 1B, albumin), but detectable by RT-PCR (not shown). Glycogen was also undetected (Fig. 1B, glycogen).

By E5 (H&H stage 26), the second lobe began to form (Fig. 1B, isolated liver, arrow). At this stage, the unorganized hepatocyte precursors formed groups of tightly adhered cells surrounded by spindle shaped endothelial cells (Fig. 1B, arrow in H&E). The loosely organized hepatocyte precursors then arranged to become acini and eventually organized into tube-like hepatic cords (Fig. 1B, H&E, also see Fig. 8B). At the center of the liver lobe, moderate albumin expression surrounding the vitelline blood vessel started to be observed. Albumin was not detected in the periphery at this stage (Fig. 1B, albumin).

By E6 (H&H stage 28), the second lobe had formed and hepatocytes became more organized, forming smaller sinusoidal spaces close to the vitelline blood channel (Fig. 1B, H&E and arrowhead). Larger sinusoidal spaces remained at the periphery and growing tip (Fig. 1B, H&E and asterisk). More tightly organized parenchymal cells were observed, possibly through interactions with the spindle shape endothelial cells (Fig. 1B, H&E and arrow). Albumin expression levels increased and expanded but still remained low at the growing tip and the periphery (Fig. 1B, albumin and arrow). Glycogen was not detected at the periphery yet, but started to become positive at the center (Fig. 1B, glycogen, E6).

By E7 (H&H stage 29), the third lobe formed as a tiny bud, ventral to the second lobe (not shown). Histologically, the structure was similar to that seen at E6 but the number of hepatocytes was markedly increased. The hepatic cords were more organized than at E6 (Fig. 1B, H&E). Albumin levels were higher, particularly at the center of the liver lobe (Fig. 1B, albumin). However, at the growing tip,

Fig. 6. Effects of over-expressing  $\beta$ -catenin on cell morphology, proliferation, and differentiation. (A) Sections from control (left) and RCAS- $\beta$ -catenin over-expressing livers (right) were stained by H&E and with antibodies against PCNA,  $\beta$ -catenin, L-CAM, c-Myc, vimentin, and tenascin-C. Glycogen was detected by PAS staining. The architecture of the affected livers was disrupted, and the well-organized hepatic cords in controls were not observed. Cells become rounder and less differentiated. The border of the liver is marked by a yellow dotted line. (B) The constitutive activity of  $\beta$ -catenin was tested with TCF-4 binding element (TBE)-linked luciferase. The plasmids were transfected into liver cells with or without RCAS- $\beta$ -catenin. The constitutively active  $\beta$ -catenin gave a markedly high expression level of luciferase. Mut-TBE + LacZ = the liver cells transfected with mutant TCF-luciferase and the control RCAS-LacZ plasmids; and WT-TBE + LacZ = liver cells transfected with wild-type TCF-luciferase and the control RCAS-LacZ plasmids. Mut-TBE +  $\beta$ -Cat = liver cells transfected with mutant TCF-luciferase and RCAS- $\beta$ -catenin plasmids; WT-TBE +  $\beta$ -Cat = the liver cells transfected with wild-type TCF-luciferase and RCAS- $\beta$ -catenin plasmids.





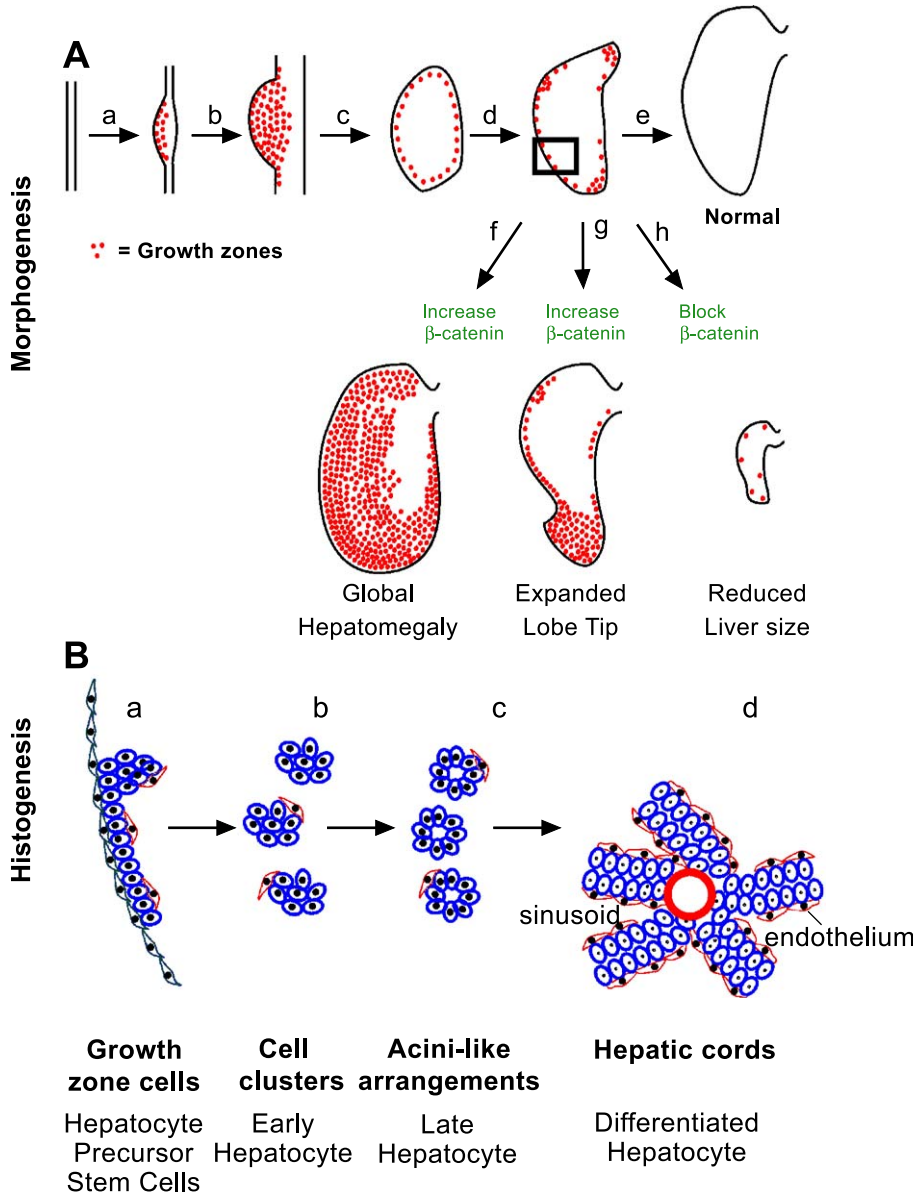


Fig. 8.  $\beta$ -catenin in the morphogenesis and histogenesis of the liver. (A) Morphogenesis. Schematic showing the distribution of  $\beta$ -catenin corresponds to the LoGZ.  $\beta$ -Catenin expression was up-regulated where the liver was induced at E2 (a), increased throughout the liver bud at E4 (b), shifted to the periphery at about E6 (c), and then became restricted to specific growth zones at about E8 (d). The strategic location of LoGZ can influence the shape and size of the liver (e). Elevated expression of  $\beta$ -catenin leads to overall enlarged livers (f) or an expanded growth tip (g, less frequency). Blocking  $\beta$ -catenin activity leads to a reduction in size of the liver (h). (B) Histogenesis. Schematic diagram shows the arrangement of hepatocytes and precursors (blue color) from the periphery to the center of the liver (in the indicated rectangular area from A). At the periphery in the LoGZ, the proliferating hepatocyte precursors are not yet organized and are flanked by an outside layer of flat layer cells (green) and an inside layer of mesenchymal cells (red color) (a). At stage b, cell clusters begin to form and are organized into acini in the subperipheral area (c). Toward the center the liver, the hepatocytes are organized into hepatic cords and the cords are sandwiched by endothelial cells (d).

albumin expression levels remained low. The level of glycogen at the center of liver lobe was increased by E8 and became ubiquitous in the liver lobe at E15 (Fig. 1B,

glycogen). These data suggest that differentiation started at the center of the liver lobe and gradually expanded to the periphery.

Fig. 7. Effects of blocking  $\beta$ -catenin activity by DKK and DNLEF1 in developing chicken liver. (A) Livers from controls, RCAS-DNLEF1, and RCAS-DKK. The diagram on the right shows the comparison of weights ( $n = 5$ ). (B) Effects of blocking  $\beta$ -catenin on cell morphology, proliferation, and differentiation. Sections from control (left), RCAS-DNLEF1 (middle), and RCAS-DKK (right) were analyzed with H&E and stained with antibodies against PCNA,  $\beta$ -catenin, and L-CAM. Presence of glycogen and TUNEL were also analyzed. To verify viral transduction, the same areas analyzed for RCAS-DNLEF1 and RCAS-DKK were also stained with antibody 3C2 to viral protein, and antibodies to HA tag on RCAS-DKK.

### Identification of proliferative zones during liver development

The distribution of growth zones was next examined using a cell proliferative marker, PCNA. Interestingly, it shows a reciprocal expression pattern to that of albumin/glycogen. The antibody to PCNA first showed nuclear positive cells throughout the liver lobe at E4 (Fig. 2, E4). By E6, PCNA gradually became negative in the center of the liver and proliferating cells were detected at the periphery and growing tip of the liver lobe (Fig. 2, E6). By E8, the peripheral growth zone started fragmenting with some segments devoid of proliferating cells (Fig. 2, Peri2) and others with more proliferating cells (Fig. 2, Peri1, Apex).

To trace the lineage of cells in the growth zone, DiI was used. DiI was injected into the surface of the developing liver primordia at E4 or E5 in ovo. At different times, livers were removed and examined by confocal microscopy. While some labeled cells remain at the injection site, most labeled cells shift positions toward the center, resulting from a possible combination of cell proliferation and migration (Fig. 3). It is consistent with the thought that cells in the peripheral growth zone give rise to cells in the parenchyma, although it does not rule out that parenchymal cells can also be generated elsewhere.

### Molecular profile of the LoGZ

Next, in situ hybridization and immunostaining were used to see what molecules are expressed in the growth zones. L-CAM, vimentin, tenascin-C, and  $\beta$ -catenin were expressed in interesting patterns. At E4, L-CAM (E-cadherin) was detected in the cytoplasm and cell membrane of the parenchyma. At E6, L-CAM was seen in the cell membrane and was more intense in the periphery than the center of the liver (Gallin et al., 1983). At E8, staining continued to be more intense in the periphery than in the center and almost absent in the non-LoGZ (Fig. 4A). In general, in LoGZ, L-CAM is present in higher amounts and is in both cytoplasm and cell membrane. In the parenchyma and in the non-LoGZ periphery, L-CAM is present in membrane form and more in the intercellular junctions.

Livers were then stained with mesenchymal cell markers to test their involvement in LoGZ activity. Interestingly, the growth zone hepatocyte precursors were sandwiched by two layers of mesenchymal cells that stain with vimentin and tenascin-C. At E4, vimentin was intense in the peripheral mesenchyme. At E6 and E8, vimentin is present in some intra-hepatic flattened mesenchymal cells surrounding the parenchyma, including putative endothelial cells. It is absent in the peripheral mesenchyme where the localized growth zone disappeared at E8 (Fig. 4A). Tenascin-C, at E4, was weak and random, but absent in the peripheral mesenchyme that was positive for vimentin. At E6, tenascin clearly demarcated the peripheral growth zone by being present as a lamina on the side of the hepatocyte precursors that face

the liver center (Fig. 4A). Tenascin-C was absent in the endothelium and other central areas. At E8, the characteristic tenascin expression pattern remained only in the mesenchymal cells of localized growth zone regions, but was completely negative in non-growth zone regions (Fig. 4A). At later stages, such as E15, the expression was absent in both growth and non-growth zones. Fibronectin was present in both the peripheral and inward mesenchymal cells. However, its presence was more ubiquitous and was present in both growth zone and non-growth zone regions (Table 1).

Among the many molecules analyzed by in situ hybridization,  $\beta$ -catenin was the major species that co-localizes and co-shifts with the localized growth zones. At E4,  $\beta$ -catenin mRNA was detected uniformly throughout the liver bud (Fig. 4B). At E5, the expression pattern gradually decreased in the center but remained at high levels in the periphery of the liver lobe (Fig. 4B). At E7,  $\beta$ -catenin expression was strongly localized to the periphery particularly at the growing tip when compared to the center area (Fig. 4B, small rectangular for center).

$\beta$ -catenin protein was next detected by immunostaining (Fig. 4C). At E4,  $\beta$ -catenin was throughout the liver lobe. At E6,  $\beta$ -catenin was detected strongly in the periphery but became negative in the center. At E8,  $\beta$ -catenin was expressed in parts of the periphery, enriched in the apex and some of the periphery regions, but negative in some other periphery regions. Subcellularly,  $\beta$ -catenin is present in the membrane, cytoplasmic and nuclear regions. The diffuse cytoplasmic staining has dampened the nuclear staining appearance. Although not present in every cell, nuclear staining was observed (Fig. 4C, inset). In some regions, membrane staining is more intense between cells than on free cell surfaces, similar to L-CAM at this stage.

As  $\beta$ -catenin is downstream to some Wnt members, we also examined their expression. We detected Wnt 3a and Wnt 8b in the localized growth zone (Wnt 3a is shown in Fig. 4D, Wnt 8b has similar pattern and is not shown). The activity of these Wnts are known to be mediated through the canonical pathway (Kengaku et al., 1998; Saitoh et al., 2002). On the other hand, Wnt 5a and Wnt 11 are also detected in the developing liver, but diffusely in both the periphery and center (not shown). The activities of Wnt 5a and 11 are known to be mediated through the non-canonical pathways (Pandur et al., 2002; Weeraratna et al., 2002).

Table 1  
Molecular expression in localized growth zone of the liver

	$\beta$ -Catenin	Vimentin	L-CAM	Tn-C <sup>a</sup>	Fibronectin <sup>a</sup>
Outermost mesenchyme	+	+	–	–	+
Growth zone cells	+	–	+	–	–
Intra-hepatic mesenchyme	–	+	–	+	+

<sup>a</sup> Fibronectin was also present in the non-growth zones, but tenascin-C was only in the localized growth zones.

Thus,  $\beta$ -catenin and some of the Wnts, which induce the canonical pathway member, are co-localized with the LoGZ.

*Overexpression of  $\beta$ -catenin produces enlarged livers with an expanded pool of hepatocyte precursors*

To test the role of  $\beta$ -catenin in liver growth,  $\beta$ -catenin function was examined by introducing an exogenous, constitutively active  $\beta$ -catenin to chicken embryos using the RCAS retroviral vector (Figs. 5A, B). Virus was injected into the body cavity between the heart and gizzard where the liver starts at E3. The presence of virus introduced into the livers as confirmed by RT-PCR in isolated affected livers (Figs. 5C, D) and by staining for anti-AMV-3C2 (similar result as Fig. 7B, 3C2).

The major phenotype observed is the enlargement of the liver at both E10 and E15 (Fig. 5A). The livers from the affected embryos contained more mass than the controls (Fig. 5E). The approximate weight increase was between 1.5- and 5-fold with  $P < 0.05$ . Some embryos with high infection show severe phenotypes and die prematurely before E15.

Next, the effects of ectopic  $\beta$ -catenin expression on hepatocyte morphology, cell proliferation, and differentiation were determined. E15 affected livers were analyzed (Fig. 6A). Similar results were obtained from other stages examined. Morphologically, the transduced hepatocytes resembled those cells from normal livers at earlier stages (E4 or E5) and cells in the LoGZ later (E7, E8). The cells were either round or cuboidal, and the nucleus to cytoplasm ratio (v/v) increased compared to controls. They were arranged loosely and not well organized. While there were no signs of tumor formation, the accumulation of these cells disrupted normal hepatic cord formation. PCNA staining showed proliferation localized to the periphery of control livers, but more widely distributed in both the periphery and the parenchyma of transduced livers. Similarly,  $\beta$ -catenin is now present not only in the periphery but also as patches in regions of the parenchyma. The staining pattern changed from higher in the membrane to higher in the cytoplasm and nucleus.

L-CAM expression was also changed from a membrane-staining pattern to a cytoplasmic expression pattern, similar to those observed in undifferentiated hepatocytes at earlier times, such as E4 (Fig. 4A). c-Myc, normally present very weakly in the periphery, now was strongly expressed in patchy regions of both the periphery and parenchyma. c-Myc is known to be downstream to  $\beta$ -catenin (Ishigaki et al., 2002). Vimentin expressing mesenchymal/endothelial cells were increased, but they were not as well organized as the controls, which formed nice sinusoidal spaces (Fig. 6A). Tenascin expression persisted in the periphery but become more diffusely expressed (Fig. 6A). Glycogen was diminished in affected livers compared to controls (Fig. 6A), suggesting that differentiation is inhibited in livers ectopically expressing constitutively active  $\beta$ -catenin. These

results imply that hepatocytes may remain at an early precursor stage and do not differentiate appropriately in the presence of excess  $\beta$ -catenin activity.

To determine whether the canonical  $\beta$ -catenin signaling pathway was active in these transduced cells, a TCF binding element (TBE) promoter–luciferase reporter construct was used (He et al., 1998). The results showed much higher activity in RCAS  $\beta$ -catenin-transduced specimens (Fig. 6B). Together, these data suggest that ectopic  $\beta$ -catenin expression increased the proliferation potential of transduced cells, and the characteristics of these cells are similar to that of the LoGZ.

*Suppression of  $\beta$ -catenin/Wnt pathway leads to small livers with under-developed hepatocytes*

In contrast, in the loss of function studies, the affected livers showed the opposite results. Both RCAS-DNLEF1 and RCAS-DKK dramatically decreased the size and altered the shape of the livers (Fig. 7F;  $n = 9$  and 6). The weights of affected embryos were compared at E13 (Fig. 7A, diagram;  $n = 3$  and 2, respectively).

The liver cells in both RCAS-DNLEF1- and RCAS-DKK-affected livers seemed to have disruption of hepatic cord structure and failed to form sinusoidal spaces (Fig. 7B). Both affected livers showed decreased cell proliferation (judged by PCNA staining) and increased TUNEL-positive cells. This is consistent with the report that DNLEF1 was shown to induce caspase expression and apoptosis (Chen et al., 2003). The hepatocytes show reduced L-CAM expression. They do differentiate to express glycogen, but the staining was not as uniform as in the control. Therefore, blocking the canonical  $\beta$ -catenin activity may have depleted hepatocyte precursor cell pools by a loss of balance among proliferation, differentiation, and apoptosis (Zechner et al., 2003), which resulted in smaller and unusual-shaped liver lobes.

## Discussion

Liver development can be studied at the level of morphogenesis and histogenesis. Initially all liver cells had a high proliferation rate, presumably to generate cells for liver primordia formation. In mice, the primordia invade the surrounding mesenchymal cells of the septum transversum and expand (Le Douarin, 1975; Rossi et al., 2001). In zebrafish, the liver cells aggregate and proliferate to form a liver bud (Field et al., 2003). In this work, we set out to study how new cells are added to the developing liver, and what molecular pathways may be involved using the chicken model. The study is consistent with the hypothesis that newly generated hepatocyte precursors are added to the outer layer of the primordia and later, at places where LoGZ activities remain. With both overexpressing and functional blocking studies, we showed  $\beta$ -catenin plays a critical role

in keeping the LoGZ active, that is, keeping the hepatocyte precursors in a proliferative and undifferentiated status longer, and thereby enlarging liver mass in those loci. Indeed, blocking  $\beta$ -catenin activity resulted in much smaller-sized livers with a depletion of the hepatocyte precursors.

#### *Identifying the dynamically shifting growth zones during chicken liver development*

In general, organ morphogenesis relies on the temporal and spatial distribution of cell proliferation, cell adhesion, cell death, cell differentiation, and cell organization. For example, the localized growth zone in the limb bud is in the distal limb bud and the duration of its activity determines the length of the limb (Johnson and Tabin, 1997; Tickle and Wolpert, 2002). In feathers, the growth zones are first localized in the distal feather bud, then become proximally located in the follicle, and finally reside in the barb ridge. Thus, LoGZ helps to build the shape of skin appendages by adding cells at specific locations at specific times (Chodanekar et al., 2002; Chuong et al., 2000).

The liver has a peculiar but reproducible shape and size (Gumucio et al., 1996). If all cells in the developing liver have the same proliferative rate, the liver would end up with a ball-like morphology, as seen in some hepatomas. Since this is not the case, there must be some differential growth based on the LoGZ in the developing liver. The liver LoGZ has not been identified or characterized. Therefore, we focused on identifying these LoGZ and characterizing their molecular basis and roles in liver development. At particular stages during liver development, the liver mass seems to be controlled precisely and tightly (reviewed in Michalopoulos, 1990, our unpublished data for chicken). However, some regions grow unevenly, producing the characteristic shape of liver lobes. In regions where LoGZ activity is maintained, a layer of proliferating hepatocytes is left at the periphery and the liver lobe will expand in this locus. By E7, the LoGZ became “segmented” and was more prominent in the ventral versus the dorsal surface. These results support the model that the spatial and temporal positioning of the LoGZ in the developing liver primordia helps to define the final shape and size of the liver.

#### *$\beta$ -Catenin maintains the activity of the LoGZ that modulates the liver size*

$\beta$ -Catenin regulates cell proliferation (Monga et al., 2003; Orford et al., 1999). The expression pattern of  $\beta$ -catenin was initially all over the liver, then became limited to the periphery, and finally became restricted to the liver lobe tips. This parallels the shifting LoGZ activity (Fig. 8A). Therefore, it is reasonable to hypothesize that the  $\beta$ -catenin pathway is involved in the function of the LoGZ. We postulate that  $\beta$ -catenin acts as an activator of proliferation during early hepatogenesis to establish the liver mass. In the

LoGZ, immunostaining showed that  $\beta$ -catenin protein is localized in the cell membrane, cytoplasm, and nucleus. They appear to reach equilibrium without dominant nuclear staining, suggesting that the role of  $\beta$ -catenin here is both adhesion and transcriptional. In the more mature liver parenchyma cells toward the center,  $\beta$ -catenin protein was much stronger in the cell membrane, suggesting the predominant function here may be related to cell adhesion, such as the rearrangement of hepatoblasts into liver cords. In the most mature hepatocytes,  $\beta$ -catenin staining disappears. At E8, regions of strong  $\beta$ -catenin expression became restricted to the tip and some segments of the developing lobes.

In the present work, we were able to test the specific roles of  $\beta$ -catenin using the chicken model. Overall, the liver can increase 3-fold in weight by overexpressing  $\beta$ -catenin. In some cases, it leads to the formation of an expanded lobe. Analyses showed that expanded cell populations are highly positive for PCNA, c-Myc, but lack glycogen. These data combined with the enhanced expression of L-CAM suggest that these cells may represent an expanded pool of early hepatocyte precursors. These cells did not resemble tumor cells because they did not show abnormal mitosis, locus formation, or invasion.

The ability of  $\beta$ -catenin to increase cell proliferation has been shown. In the mouse, suppression of  $\beta$ -catenin reduced liver cell proliferation (Monga et al., 2003).  $\beta$ -Catenin in conjunction with a LEF/Tcf co-transcription activator induces c-Myc and cyclin-D1 expression (Utsunomiya et al., 2001), hence increasing cell number. Transgenic mice, expressing a stabilized  $\beta$ -catenin form from an endolase promoter, gave rise to hepatomegaly (Cadoret et al., 2001). Additionally,  $\beta$ -catenin expressed from adenovirus was shown to cause hepatomegaly (Harada et al., 2002). During liver regeneration,  $\beta$ -catenin promotes proliferation required to restore liver mass after partial hepatectomy (Monga et al., 2001). Indeed, liver cell proliferation was shown to be dependent on the expression of  $\beta$ -catenin in vitro (Monga et al., 2003). While  $\beta$ -catenin may be important for liver growth, the deregulation of its activity can lead to carcinogenesis. Mis-regulation of  $\beta$ -catenin has been shown to lead to transformation and tumorigenesis (Polakis, 2000). In contrast, reducing  $\beta$ -catenin activity by DN-LEF1 or DKK led to a reduction in liver size. Pathological analyses showed reduced cell proliferation, and affected cells are defective in their control of growth, apoptosis, and differentiation.

#### *Micro-environment of localized growth zone and histogenesis of the liver*

Hepatocyte precursor cells proliferate in the growth zone, and are sandwiched by the mesothelial cells on the outside and tenascin-C positive mesenchymal cells inside (Fig. 8B). When a certain threshold is reached, cells start to arrange themselves and progress toward differentiated hepatocytes, while cells remaining in the growth zone still express higher

$\beta$ -catenin levels, retain their high proliferation rate and possible pluripotentiality. Thus new cells are added to the outer layer of the primordia, and the whole liver lobe continues to grow in size.

How are cell fates in the growth zone regulated? We contend that growth control is regulated by epithelial–mesenchymal interactions between the growth zone hepatocytes and the adjacent two types of mesenchymal cells. When ready, hepatocyte precursors generate cells that may leave the growth zone that are displaced inward. Our DiI-labeled experiments are consistent with this proposed transition. These early hepatoblasts are progressively organized first into acini, then into a cord configuration (Fig. 8B). This must involve changes in adhesion molecules. For example, tenascin-C positive mesenchymal cells are selectively high beneath the growth zone cells but are absent in regions where growth has subsided. Tenascin has been shown to be a de-adhesion molecule and may play a role to allow cell rearrangement and active morphogenesis (Murphy-Ullrich, 2001).

L-CAM (chicken E cadherin; Gallin et al., 1983) is detected in both the cytoplasm and cell membrane of hepatocyte precursors in the LoGZ. Since the cytoplasmic E-cadherin domain can bind  $\beta$ -catenin, it is possible that L-CAM expression also helps to regulate the level of  $\beta$ -catenin by binding to its cytoplasmic tail, hence modulating the  $\beta$ -catenin pool. In the parenchymal cells immediately subjacent to the growth zone, both L-CAM and  $\beta$ -catenin become intensified at sites with cell–cell surface interactions and reduced in free cell surfaces. This change of cell adhesion allows cells to move from a homogenous adhesive environment to one with enhanced adhesion in polarized subcellular regions (Sorkin et al., 1991). It is probably a prelude to cellular rearrangements required to build the liver architecture (Jamora et al., 2003). Indeed, overexpressing DN-LEF1 or DKK could turn off the expression of L-CAM and resulted in a lack of hepatic cord formation.

The elongations of the limb and feather are driven by specific localized growth zones. In this work, we show that the expansion of the liver is also driven by temporally and spatially specific growth zone activity. We further showed the activity of  $\beta$ -catenin is critical for this activity. However, there are likely to be more molecules involved in regulating this growth zone activity. The current work sets the groundwork for these future studies.

## Acknowledgments

We thank Mr. David Huang for help in this work and Ms. Maji Ramos and Fiona McCulloch for the preparation of the manuscript; Dr. Neil Kaplowitz and Dr. Hide Tsukamoto for constructive comments and support; and Joe Lin and Zhicao Yue for discussions in solving technical problems. We are grateful to Dr. Randy Johnson for RCAS  $\beta$ -catenin, Dr. Tabin for DN-LEF1, Dr. Andrew Lassar and Dr. Sarah Millar for DKK, and Dr. William Pavan for RCAS Gateway

cloning vector. This study was supported by grants from NIDDK P30 DK048522 (the USC Research Center for Liver Diseases), NIH AR42177, AR47364 (CMC), and NCI CA83716 (RW). Sanong Suksaweang is supported by the Royal Thai Government Scholarship from Thailand.

## References

- Cadoret, A., Ovejero, C., Saadi-Kheddouci, S., Souil, E., Fabre, M., Romagnolo, B., Kahn, A., 2001. Hepatomegaly in transgenic mice expressing an oncogenic form of  $\beta$ -catenin. *Cancer Res.* 61, 3245–3249.
- Capdevila, J., Tabin, C., Johnson, R.L., 1998. Control of dorsoventral somite patterning by Wnt-1 and  $\beta$ -catenin. *Dev. Biol.* 193, 182–194.
- Carlson, B.M., 1999. Formation of the liver. *Human Embryology and Developmental Biology*. Mosby, Missouri, pp. 337–347.
- Chen, T., Yang, I., Irby, R., Shain, K.H., Wang, H.G., Quackenbush, J., Coppola, D., Cheng, J.Q., Yeatman, T.J., 2003. Regulation of caspase expression and apoptosis by adenomatous polyposis coli. *Cancer Res.* 63, 4368–4374.
- Chodankar, R., Chang, C.H., Yue, Z., Jiang, T.X., Suksaweang, S., Burrus, L.W., Chuong, C.M., Widelitz, R.B., 2002. Shift of localized growth zones contributes to skin appendage morphogenesis: role of the Wnt/ $\beta$ -catenin pathway. *JID* 120, 20–26.
- Chuong, C.M., 1998. Morphogenesis of epithelial appendages: variations on top of a common theme and implications in regeneration. In: Chuong, C.M. (Ed.), *Molecular Basis of Epithelial Appendage Morphogenesis*. R.G. Landes, Texas, pp. 1–13.
- Chuong, C.M., Chodankar, R., Widelitz, R.B., Jiang, T.X., 2000. Evo-devo of feathers and scales: building complex epithelial appendages. *Curr. Opin. Genet. Dev.* 10, 449–456.
- Field, H.A., Ober, E.A., Roeser, T., Stainier, D.Y., 2003. Formation of digestive system in zebrafish. I. Liver morphogenesis. *Dev. Biol.* 253, 279–290.
- Gallin, W.J., Edelman, G.M., Cunningham, B.A., 1983. Characterization of L-CAM, a major cell adhesion molecule from embryonic liver cells. *Proc. Natl. Acad. Sci.* 80, 1038–1042.
- Glinka, A., Wu, W., Delius, H., Monaghan, A.P., Blumenstock, C., Niehrs, C., 1998. Dickkopf-1 is a member of a new family of secreted proteins and functions in head induction. *Nature* 391, 357–362.
- Gumucio, J.J., Berkowitz, C.M., Webster, S.T., Thornton, A.J., 1996. In: Kaplowitz, N. (Ed.), *Liver and Biliary Diseases*. Williams & Wilkins, Maryland, pp. 3–19.
- Hamburger, V., Hamilton, H.L., 1951. A series of normal stages in the development of the chick embryo. *J. Morphol.* 88, 49–92 (reprinted in *Dev. Dyn.* 1992. 195, 231–272).
- Harada, N., Miyoshi, H., Murai, N., Oshima, H., Tamai, Y., Oshima, M., Taketo, M.M., 2002. Lack of tumorigenesis in the mouse liver after adenovirus-mediated expression of a dominant stable mutant of  $\beta$ -catenin. *Cancer Res.* 62, 1971–1977.
- He, T.-C., Sparks, A.B., Rago, C., Hermeking, H., Zawel, L., Costa, L.T., Morin, P.J., Vogelstein, B., Kinzler, K.W., 1998. Identification of c-Myc as a target of the APC pathway. *Science* 281, 1509–1512.
- Hogan, B.L.M., 1999. Morphogenesis. *Cell* 96, 225–233.
- Ishigaki, K., Namba, H., Nakashima, M., Nakayama, T., Mitsutake, N., Hayashi, T., Maeda, S., Ichinose, M., Kanematsu, T., Yamashita, S., 2002. Aberrant localization of beta-catenin correlates with over-expression of its target gene in human papillary thyroid cancer. *J. Clin. Endocrinol. Metab.* 87, 3433–3440.
- Jamora, C., DasGupta, R., Kocieniewski, P., Fuchs, E., 2003. Links between signal transduction, transcription and adhesion in epithelial bud development. *Nature* 422, 317–322.
- Jeng, Y.M., Wu, M.Z., Mao, T.L., Chang, M.H., Hsu, H.C., 2000. Somatic mutations of  $\beta$ -catenin play a crucial role in the tumorigenesis of sporadic hepatoblastoma. *Cancer Lett.* 152, 45–51.

- Jiang, T.X., Stott, N.S., Widelitz, R.B., Chuong, C.M., 1998. Current methods in the study of avian skin appendages. In: Chuong, C.M. (Ed.), *Molecular Basis of Epithelial Appendage Morphogenesis*. R.G. Landes Co., Texas, pp. 395–408.
- Johnson, R.L., Tabin, C.J., 1997. Molecular models for vertebrate limb development. *Cell* 90, 979–990.
- Jung, J., Zheng, M., Goldfarb, M., Zaret, K.S., 1999. Initiation of mammalian liver development from endoderm by fibroblast growth factors. *Science* 284, 1998–2002.
- Kengaku, M., Capdevila, J., Rodriguez-Esteban, C., De La Pena, J., Johnson, R.L., Belmonte, J.C.I., Tabin, C.J., 1998. Distinct WNT pathways regulating AER formation and dorsoventral polarity in the chick limb bud. *Science* 280, 1274–1277.
- Le Douarin, N.M., 1975. An experimental analysis of liver development. *Med. Biol.* 53, 427–455.
- Loftus, S.K., Larson, D.M., Watkins-Chow, D., Church, D.M., Pavan, W.J., 2001. Generation of RCAS vectors useful for functional genomic analyses. *DNA Res.* 8, 221–226.
- Lu, J., Chuong, C.M., Widelitz, R.B., 1997. Isolation and characterization of chicken  $\beta$ -catenin. *Gene* 196, 201–207.
- Michalopoulos, G.K., 1990. Liver regeneration: molecular mechanisms of growth control. *FASEB J.* 4, 176–187.
- Monga, S.P., Padiaditakis, P., Mule, K., Stolz, D.B., Michalopoulos, G.K., 2001. Changes in Wnt/ $\beta$ -catenin pathway during regulated growth in rat liver regeneration. *Hepatology* 33, 1098–1109.
- Monga, S.P., Monga, H.K., Tan, X., Mule, K., Padiaditakis, P., Michalopoulos, G.K., 2003.  $\beta$ -Catenin antisense studies in embryonic liver cultures: role in proliferation, apoptosis, and lineage specification. *Gastroenterology* 124, 202–216.
- Murphy-Ullrich, J.E., 2001. The de-adhesive activity of matricellular proteins: is intermediate cell adhesion an adaptive state? *J. Clin. Invest.* 107, 785–790.
- Orford, K., Orford, C.C., Byers, S.W., 1999. Exogenous expression of  $\beta$ -catenin regulates contact inhibition, anchorage-independent growth, anoikis, and radiation-induced cell cycle arrest. *J. Cell Biol.* 146, 855–867.
- Pandur, P., Lasche, M., Eisenberg, L.M., Kuhl, M., 2002. Wnt-11 activation of a non-canonical Wnt signalling pathway is required for cardiogenesis. *Nature* 418, 636–641.
- Polakis, P., 2000. Wnt signaling and cancer. *Genes Dev.* 14, 1837–1851.
- Rossi, J.M., Dunn, N.R., Hogan, B.L.M., Zaret, K.S., 2001. Distinct mesodermal signals, including BMPs from the septum transversum mesenchyme, are required in combination for hepatogenesis from the endoderm. *Genes Dev.* 15, 1998–2009.
- Saito, T., Oda, Y., Sakamoto, A., Tamiya, S., Kinukawa, N., Hayashi, K., Iwamoto, Y., Tsuneyoshi, M., 2000. Prognostic value of the preserved expression of the E-cadherin and catenin families of adhesion molecules and of  $\beta$ -catenin mutations in synovial sarcoma. *J. Pathol.* 192, 342–350.
- Saitoh, T., Mine, T., Katoh, M., 2002. Expression and regulation of WNT8A and WNT8B mRNAs in human tumor cell lines: up regulation of WNT8B mRNA by beta-estradiol in MCF-7 cells, and down-regulation of WNT8A and WNT 8B mRNAs by retinoic acid in NT2 cells. *Int. J. Oncol.* 20, 999–1003.
- Sorkin, B.C., Gallin, W.J., Edelman, G.M., Cunningham, B.A., 1991. Genes for two calcium-dependent cell adhesion molecules have similar structures and are arranged in tandem in the chicken genome. *Proc. Natl. Acad. Sci.* 88, 11545–11549.
- Tickle, C., Wolpert, L., 2002. The progress zone—Alive or dead? *Nat. Cell Biol.* 4, E216–E217.
- Utsunomiya, T., Doki, Y., Takemoto, H., Shiozaki, H., Yano, M., Sekimoto, M., Tamura, S., Yasuda, T., Fujiwara, Y., Monden, M., 2001. Correlation of beta-catenin and cyclin D1 expression in colon cancers. *Oncology* 61, 226–233.
- Vessey, C.J., Hall, P.M., 2001. Hepatic stem cells: a review. *Pathology* 33, 130–141.
- Wang, X., Montini, E., Al-Dhalimy, M., Lagasse, E., Finegold, M., Grompe, M., 2002. Kinetics of liver repopulation after bone marrow transplantation. *Am. J. Pathol.* 161, 565–574.
- Warren, M.F., Hamilton, P.B., 1981. Glycogen storage disease type X caused by ochratoxin A in broiler chickens. *Poult. Sci.* 60, 120–123.
- Weeraratna, A.T., Jiang, Y., Hostetter, G., Rosenblatt, K., Duray, P., Bittner, M., Trent, J.M., 2002. Wnt5a signaling directly affects cell motility and invasion of metastatic melanoma. *Cancer Cells* 1, 279–288.
- Wei, Y., Fabre, M., Branchereau, S., Gauthier, F., Perilongo, G., Buendia, M.A., 2000. Activation of beta-catenin in epithelial and mesenchymal hepatoblastomas. *Oncogene* 19, 498–504.
- Widelitz, R.B., Jiang, T.X., Lu, J., Chuong, C.M., 2000.  $\beta$ -Catenin in epithelial morphogenesis: conversion of part of avian foot scales into feather buds with a mutated  $\beta$ -catenin. *Dev. Biol.* 219, 98–114.
- Zaret, K.S., 2000. Liver specification and early morphogenesis. *Mech. Dev.* 92, 83–88.
- Zaret, K.S., 2002. Regulatory phases of early liver development: paradigms of organogenesis. *Nat. Rev., Genet.* 3, 499–512.
- Zechner, D., Fujita, Y., Hulsken, J., Muller, T., Walter, I., Taketo, M.M., Crenshaw III, E.B., Birchmeier, W., Birchmeier, C., 2003.  $\beta$ -Catenin signals regulate cell growth and the balance between progenitor cell expansion and differentiation in the nervous system. *Dev. Biol.* 258, 406–418.